Effects of Star Formation Stochasticity on the Lyα & Lyman Continuum Emission from Dwarf Galaxies during Reionization

Jaime E. Forero-Romero[1] ⋆ and Mark Dijkstra[2]

[1] *Department of Astronomy, University of California, Berkeley, CA 94720-3411, USA*
[2] *Max-Planck Institut fuer Astrophysik, Karl-Schwarzschild-Str. 1, 85741 Garching, Germany*

19 October 2012

ABSTRACT
Observations of distant galaxies play a key role in improving our understanding of the Epoch of Reionization (EoR). The observed Lyα emission line strength – quantified by its restframe equivalent width (EW) – provides a valuable diagnostic of stellar populations and dust in galaxies during and after the EoR. In this paper we quantify the effects of star formation stochasticity on the predicted Lyα EW in dwarf galaxies, using the publicly available code SLUG (used to 'Stochastically Light Up Galaxies'). We compute the number of hydrogen ionizing photons, as well as flux in the Far UV for a set of models with star formation rates (SFR) in the range 10^{-3}-1 $M_\odot$ yr^{-1}. From these fluxes we compute the luminosity, L_α, and the EW of the Lyα line. We find that stochasticity alone induces a broad distribution in L_α and EW at a fixed SFR, and that the widths of these distributions decrease with increasing SFR. We parameterize the EW probability density function (PDF) as an SFR–dependent double power law. We find that it is possible to have EW as low as $\sim$EW$_0$/4 and as high as $\sim 3\times$EW$_0$, where EW$_0$ denotes the expected EW in the absence of stochasticity. We argue that stochasticity may therefore be important when linking drop-out and narrow-band selected galaxies, when identifying population III galaxies, and that it may help to explain the large EW (EW $\gtrsim$100 − 200 Å) observed for a fraction of Lyα selected galaxies. Finally, we show that stochasticity can also affect the inferred escape fraction of ionizing photons from galaxies. In particular, we argue that stochasticity may simultaneously explain the observed anomalous ratios of the Lyman continuum flux density to the (non-ionizing) UV continuum density in so-called Lyman-Bump galaxies at $z = 3.1$, as well as the absence of such objects among a sample of $z = 1.3$ drop-out galaxies.

Key words: galaxies: high-redshift - galaxies: star formation - line: formation

1 INTRODUCTION

The Epoch of Reionization (EoR) represents a milestone in the evolution of our Universe, during which hydrogen gas in most of its volume changed from fully neutral to fully ionized. Observations of the cosmic microwave background support that reionization started at redshift $z \sim 20$ while quasars observations demonstrate that the process was completed at $z \sim 5 - 6$ (e.g. Mesinger 2010; Pritchard et al. 2010). One key to new insights in this area are observations of high redshift galaxies, as they will allow for the construction of a complete physical picture of the reionization process.

Observations of distant Lyman Break Galaxies (LBGs) and Lyman α Emitters (LAEs) in the redshift range $4 < z < 10$ have provided the most prominent windows on the star formation history at these early epochs (see e.g. Robertson et al. 2010, and references therein). LBGs are galaxies that have been selected using broad-band surveys, which are sensitive to the 'Lyman break' in the spectra of star forming galaxies. This break is a consequence of typical effective temperatures of O & B stars, and of interstellar and intergalactic absorption of flux blueward of the Lyα wavelength (Steidel et al. 1996). Surveys for LBGs (or 'drop-out' galaxies) are most sensitive to UV rest-frame continuum emission of galaxies. LAEs are galaxies that have been selected from narrow-band surveys which are sensitive to high-redshift galaxies that have strong Lyα line emission

⋆ IAU Gruber Fellow, Email: forero@berkeley.edu

(e.g. Rhoads et al. 2000). The Lyα line originates in HII regions that surrounded O & B stars. As a result, the Lyα line flux (and strength) in LAEs are more directly connected to the ionizing photon budget (e.g. Schaerer 2003).

The 'strength' of the Lyman α emission line is quantified by its rest-frame equivalent width (EW), which corresponds to the ratio between the line intensity and the continuum. The Lyα EW is an important physical quantity associated with galaxies during the EoR for (at least) three reasons : (i) narrowband surveys for LAEs are typically sensitive to galaxies for which the Lyα EW exceeds some threshold value (which can range between EW$\sim 20 - 65$ Å, see e.g. Ouchi et al. 2008). The Lyα EW is clearly an important physical quantity that links the LBG and LAE populations; (ii) the 'first' galaxies that formed from pristine gas are expected to be characterised by unusually large EW (well in excess of EW~ 200 Å), which may be one of their most prominent observational signatures (Schaerer 2003; Johnson et al. 2009; Raiter et al. 2010); (iii) recent observations of LAEs & LBGs in the redshift range $z = 3 - 7$ have revealed an apparent non-monotonic evolution in the EW distribution, with significantly less Lyα being observed from galaxies beyond redshift $z > 6$ (Stark et al. 2010, 2011; Pentericci et al. 2011; Ono et al. 2012; Schenker et al. 2012).

The redshift evolution in the EW distribution at $z > 6$ is likely to be connected with the reionization process rather than with secular evolution process in the galaxies (Forero-Romero et al. 2012, also see Shimizu et al. (2011)). Although current observations do not allow for robust conclusions, analyzing EW distributions provides a powerful technique to probe the population of star forming galaxies – as well as the ionization state of the IGM – during and after reionization has been completed (e.g. Dijkstra et al. 2011, also see Dayal & Ferrara (2012)).

Recently, Fumagalli et al. (2011) showed that at low levels of star formation (SFR $< 1M_\odot$ yr^{-1}), the effects of the statistical description of the stellar Initial Mass Function (IMF) and the Cluster Mass Function (CMF) emerge. Among the expected effects – gathered under the name of 'stochasticity' – the most relevant for our discussion is that the flux ratio between ionizing and Far UV photons fluctuates around the mean expected value. Fumagalli et al. (2011) show how the clustering of star formation together with the sampling of the Initial Mass Function (IMF) cause the ratio of the Hα flux and FUV flux density to fluctuate around the mean significantly for local dwarf galaxies. This effect should be also noticeable in the ratio of Lyα flux to FUV flux density i.e. the EW. In other words, stochasticity may affect the *intrinsic* Lyα EW-PDFs of faint LBGs ($-18 \lesssim M_{\rm UV} \lesssim -13$). Because Ly$\alpha$ EW plays an important role in understanding high–redshift galaxy populations and constraining the reionization process, it is important to understand quantitatively the impact of stochasticity.

Furthermore, observational constraints on the 'escape fraction' of ionizing photons from star forming galaxies are derived from the observed ratio of LyC flux density to FUV flux density, which is subject to the clustering of star formation and stochastic sampling of the IMF, especially at SFR $\lesssim 1$ $M_\odot$ yr^{-1}. It has long been realized that such galaxies can provide the bulk of the ionizing photons needed to reionize the IGM and to maintain it ionized (at a fixed escape fraction, see e.g. Fig 31 of Barkana & Loeb 2001). A

more recent analysis by Kuhlen & Faucher-Giguere (2012) echoes these findings. Kuhlen & Faucher-Giguere (2012) show that in plausible scenarios for reionization, star forming galaxies with very faint magnitudes $M_{\rm lim} \sim -13$ (corresponding to SFR $\sim 10^{-2} M_\odot {\rm yr}^{-1}$) contribute significantly to the overall budget of ionizing photons. While high–redshift galaxies with such low star formation rates remain too faint to be detected even by future facilities, the observation of galaxies with SFRs$= 10^{-2} - 1$ $M_\odot$ yr^{-1} at lower redshifts $z < 4$ can help us to understand the physics of such systems. For instance, the escape fraction of ionizing photons from galaxies with SFR within the upper end of that range have already been constrained by observations at $z \sim 3.0$ (Iwata et al. 2009, who constrained the escape fraction down to SFR$\sim 1 M_\odot$ yr^{-1}). The possible dependence of these estimates on stochasticity provides an additional motivation to study the consequences of the stochastic sampling of the IMF.

In this paper we set out to quantify the effects of stochasticity in the EW distribution of dwarf Lyα emitting galaxies. We implement highly simplified models for dwarf galaxies at high redshift to isolate the stochastic effect. The SFH is constant, single metallicity, without any extinction effects. We stress that our objective is not to explain or interpret current observations of LAEs and LBGs, but instead simply to isolate and highlight the impact of stochasticity on predicted values for the Lyα EW.

This paper is structured as follows. In §2 we summarize the expected effects on the equivalent width stochasticity and present the numerical experiments we perform to quantify this effect. In §3 we present the raw results that help us in §4 to asses the impact of stochasticity in different aspects of the interpretation of observations of LAEs and LBGs at high redshift. Finally, we summarize our conclusions in §5

Throughout this paper we will study the 'Lyman continuum' ($\lambda \sim 700$Å), ionizing continuum ($\lambda < 912$Å), and Far UV (FUV) continuum (~ 1500Å), where all wavelengths are rest frame. Whenever we refer to UV we imply FUV. Also, the Lyα equivalent widths are measured in the galaxies' restframe.

2   STOCHASTIC EFFECTS IN THE EQUIVALENT WIDTH

To be consistent with observations, we define the Lyα rest-frame equivalent EW as the ratio between the intensity of the Lyα line to the flux density redwards of the line[1]

$$\mathrm{EW} \equiv \frac{L_{Ly\alpha}}{L_{\lambda,UV}} = \frac{\lambda_{\rm UV}}{\nu_{\rm UV}} \frac{L_{Ly\alpha}}{L_{\nu,UV}}, \qquad (1)$$

---

[1] Formally, the equivalent width is measured relative to the flux density in the continuum just redward of the Lyα resonance, i.e. at $\lambda \sim 1216$ Å$+\epsilon$. The flux density at this wavelength is $\sim (\lambda_\alpha/\lambda_{\rm UV})^\beta$ times larger than at $\lambda_{\rm UV} = 1540$ Å, where $\beta \sim -2$ (Dunlop et al. 2012; Finkelstein et al. 2011) denotes the observed slope of the UV continuum at the redshift and UV-magnitudes of interest. Therefore, if we had corrected for the slope in the spectrum of the UV continuum, then we would have found EW$_0 \sim 70$ Å for the Kennicutt (1998) star formation calibrators (e.g. Dijkstra & Westra 2010).

where subscript ν or λ indicates the flux density in frequency or wavelength, respectively. The wavelengths and frequencies associated with the Lyα transition and the UV continuum (from the central wavelength for the filter used in SLUG) are $\lambda_\alpha = 1216$Å, $\lambda_{UV} = 1540$Å, $\nu_{Ly\alpha} = 2.47 \times 10^{15}$Hz and $\nu_{UV} = 1.97 \times 10^{15}$Hz.

We calculate the intrinsic luminosity of Lyα assuming that a fraction 0.67 of the ionizing photons are converted into Lyα. We obtain $L_{Ly\alpha} = c_0 \times Q_H$ where $c_0 = 1.04 \times 10^{-11}$ erg photon^{-1} (Schaerer 2003). We then have

$$\text{EW} = \frac{\lambda_{UV}}{\nu_{UV}} \frac{c_0 Q_H}{F_{\nu,UV}}. \tag{2}$$

In order to compare results on the same grounds results from different metallicities or star formation rates we introduce a dimensionless constant

$$\mathcal{M} \equiv \frac{\text{EW}}{\text{EW}_0}, \tag{3}$$

where EW_0 is the equivalent width expected value for high values of the star formation rate when the stochasticity effects are negligible.

We point out that under this convention $\text{EW}_0 = 96$ Å when considering a 'standard' conversion between Lyα luminosity, UV luminosity density (Kennicutt 1998), which are $L_{\nu,UV} = \text{SFR} \times 8.0 \times 10^{27}$ erg s^{-1} Hz^{-1} and $L_{Ly\alpha} = \text{SFR} \times 1.0 \times 10^{42}$ erg s^{-1}. We emphasize that an implicit assumption in the conversion is a Salpeter IMF in the mass range 0.1-100 M$_\odot$ for solar abundance. In our numerical experiments, $\text{EW}_0 = 110 \pm 12$ Å, which is a result of the lower metallicities and the higher upper limit in the IMF mass range assumed in SLUG (details are given in §2.2). These minor systematic corrections due to different conditions in stellar metallicity, IMF or star formation history won't affect our main conclusions. Throughout this paper, we will adopt $\text{EW}_0 = 110$ Å.

2.1 Stochasticity

The description of star formation is probabilistic. At its core we find the concept of the Initial Mass Function (IMF), $\phi(m)$, which describes the relative abundance of stars of a given mass to be formed. The IMF can be mostly determined by two pieces of information. The first one is the mass interval, $m_{min} - m_{max}$ that the newly formed stars can have. The second is the change of relative abundance for different stellar masses, which is usually parametrized as $\phi(m) \propto m^{-\gamma}$, if $\gamma > 0$ less massive stars are more probable to form that high mass stars.

For large masses of newly formed stars it is possible to guarantee a good sampling of the IMF. For a low rate of star formation the poor sampling of the IMF makes possible that the rarer most massive stars near m_{max} don't appear in a burst of star formation.

Star formation is also thought to proceed in clusters. This provides another important astrophysical element in the statistical description of star formation that can be impacted by stochasticity effects. In analogy to the stellar mass function, one can also parametrize the abundance of stellar clusters by the cluster mass function (CMF). Low values of

the star formation rate can also affect the sampling of the CMF.

Furthermore, stars of different mass have different evolutionary tracks. The inhomogeneous IMF sampling will produce fluctuating stellar populations with different luminosity histories, this can impact the ratio of ionizing to far UV photons produced as a function of time.

The effect of stochasticity has been explored before in the production of Hα in dwarf galaxies in the local universe (Fumagalli et al. 2011; Haas & Anders 2010), but not on the effect on the EW of Lymanα emitting galaxies. Our aim is to quantify this impact and estimate how current and future observational campaigns can be affected by these effects.

2.2 Grids of SLUG models

We used SLUG ('Stochastically Light Up Galaxies') a fully stochastic code for synthetic photometry of galaxies (Fumagalli et al. 2011; da Silva et al. 2012). The code samples the CMF and IMF of a star forming galaxy by forming individual star clusters and following their spectral evolution. At low values of a time averaged continuous SFR the series of bursts associated with the cluster formation start to be visible. Furthermore, low SFR values imply a low number of stars to sample the IMF, lowering the probability of finding massive stars. All the effects of finite sampling in mass and time have an impact on the instantaneous strength of the Lymanα emission line. SLUG assumes that a fraction f_c of the total stellar population is formed in clusters. In that case, the clusters also sample a cluster mass function(CMF) $\psi(M_{ecl}) = M_{ecl}^{-\beta}$. The stars in the cluster are then populated according to the selected IMF.

In this stochastic framework, a galaxy with a time averaged constant SFR does not level to a constant SED, but instead it continuously fluctuates in time. For a sample of independent galaxies with the same average SFR one could thus associate a distribution of line and continuum intensities.

All models used in this paper are based on a Salpeter IMF in the mass intervals 0.08–120 M$_\odot$. We consider two kinds of models of varying metallicity $Z = 4.0 \times 10^{-4}, 4.0 \times 10^{-3}$ (which corresponds to $Z = 0.02Z_\odot$, $Z = 0.2Z_\odot$). We assume that all the stars are formed in clusters, $f_c = 1$. Assuming unclustered star formation, $f_c = 0$, reduces the scatter in the flux fluctuations we report here by about an order of magnitude (da Silva et al. 2012). The CMF is described by the cluster mass interval is $20 - 10^7 M_\odot$ and the slope is $\beta = 2.0$. The stellar libraries are Padova asymptotic giant branch (AGB) tracks. The stellar Spectral Energy Distributions (SED) correspond to Lejeune et al. (1997, 1998) where the Wolf-Rayet stars treatment follows Smith et al. (2002) and Hillier & Miller (1998). We run 500 galaxies for each metallicity and star formation rate comprised in the range 10^{-3}–1 M$_\odot$/yr. Table 1 lists the exact values for the SFR and metallicity that were used. Each model runs for a period of 200 Myr with outputs every 1 Myr. Running for a period longer than 100 Myr ensures a stable base level for the mean FUV and ionizing fluxes.

We use the last 10 outputs per galaxy to slightly increase the statistical sample. Being pessimistic, one can assume that each simulated system contributes only 1 independent datum instead of 10, from that point of view, one
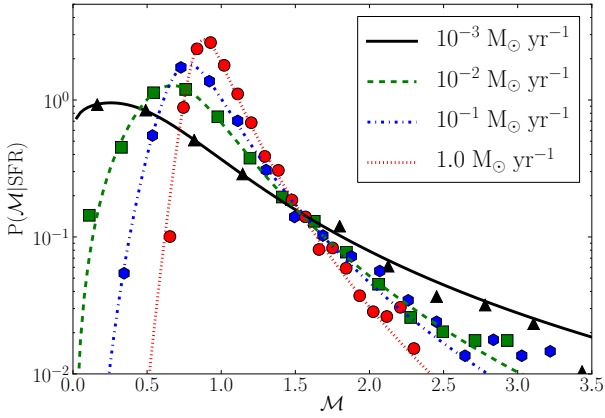
Figure 1. Different Probability Density Distributions for $\mathcal{M}$, the normalized EW. Each symbol corresponds to the binned SLUG results for a different SFR=10^{-3}, 10^{-2}, 10^{-1} and $1 M_\odot \mathrm{yr}^{-1}$ and a metallicity f $0.20 Z_\odot$. The lines are the best fit of Eq. (4) to the points.

Figure 2. Fraction of galaxies as a function of SFR that have an EW larger than a fixed value EW_c. Each line represents different threshold in $\mathrm{EW}_c = 20$, 30, 40 and 50Å . This figure quantifies the impact of the stochasticity on the fraction of confirmed LAEs based on a minimal EW detection threshold.

can be sure that all the results for the PDF and derived quantities are accurate within $1/500 \sim 0.02$. In other words, one might be concerned that the 10 outputs of the same galaxy may not be independent and might bias the PDF. To quantify this we perform the following test: for 4000 galaxies with a star formation rate 8.0×10^{-3} $M_\odot \mathrm{yr}^{-1}$ we calculate the PDF in two different ways. First by taking 10 outputs of 400 galaxies and second by using only 1 output for each one of the 4000 galaxies. We find that the absolute difference between the PDF($\mathcal{M}$) constructed from the two different samples is always on the order of ~ 0.02 and conclude that a possible bias is negligible. We perform an additional test by taking 1 output and 2 outputs for 4000 galaxies, with spectral outputs spaced by 100Myr during 500Myr and find that the difference between the PDF($\mathcal{M}$) constructed from these samples is always on the order of ~ 0.05 and conclude that a possible bias from the chosen timesteps is also negligible.

For each galaxy we obtain the flux per unit frequency $F_{\nu,\mathrm{FUV}}$ at a wavelength of 1540 Å, together with the ionizing photon rate Q_H. These quantities are used to calculate the EW as described by Eq (2). The value for EW_0 is calculated as the arithmetic average EW for 30 models of galaxies with a SFR of 5 $M_\odot \mathrm{yr}^{-1}$, we obtain $\mathrm{EW}_0 = 110 \pm 12$ where the error quoted is estimated from the standard deviation from the mean.

3 RESULTS

The net effects of stochasticity introduce a SFR dependent scatter around a central value. We describe this effect as a Probability Density Distribution (PDF) for the $\mathcal{M}$ variable. We parametrize the PDF by a double power law in order to better quantify how it depends from changes in the SFR and the metallicity,

$$P(\mathcal{M}|\mathrm{SFR}) = P_0 \left[\left(\frac{\mathcal{M}}{\mathcal{M}_0} \right)^{-\alpha} + \left(\frac{\mathcal{M}}{\mathcal{M}_0} \right)^{\gamma} \right]^{-1} . \quad (4)$$
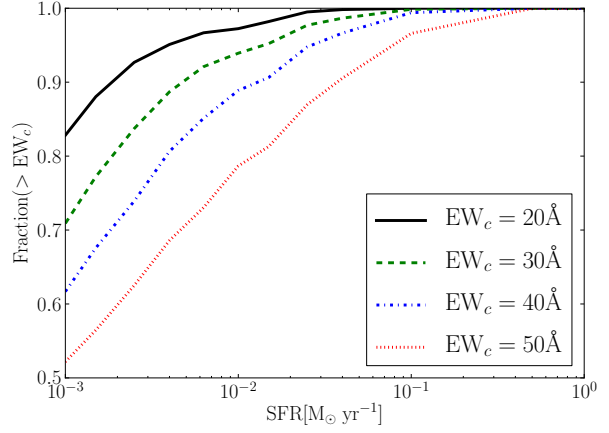
Figure 1 presents the results for the PDF $P(\mathcal{M}|\mathrm{SFR})$, the symbols represent the results from the simulations and the lines the fit to those points. Given the limited number of models the PDF is reliable only for values $P(\mathcal{M}|\mathrm{SFR}) > 10^{-2}$, likewise the deviation of the fit with respect to the simulation points is on the order of 1×10^{-2}. The star formation rate enters through the constants $\mathcal{M}_0$, α, γ, and P_0. The expected result for a perfectly sampled IMF is a delta function around M $= 1$ (Leitherer et al. 1999), while our results show a wide distribution. Each line in Figure 1 corresponds to a different SFR= 1×10^{-3}, 10^{-2}, 10^{-1} and 1.0 in units of $M_\odot \mathrm{yr}^{-1}$ for a metallicity of $0.02 Z_\odot$. The best fit values together with their uncertainty from the fitting procedure for all the SLUG models are listed in Table 1. In these values we get a precise quantification on how the PDF shape changes with the SFR. From these results we confirm that the effect of the metallicity is a second order effect shaping the EW PDF when compared to the influence of the SFR.

For high values of the SFR$> 10^{-1}$ $M_\odot \mathrm{yr}^{-1}$ the low end, $\mathcal{M} < 1$ of $P(\mathcal{M})$ increases sharply compared to the slower decrease in the high end $\mathcal{M} > 1$. In this regime the peak of the distribution is around the expected value of $\mathcal{M} = 1$ for a perfectly sampled IMF.

This quantitative behaviour presents consequences for the interpretation of high EW systems. On the upper end, on can achieve values close to what is expected to be limit of star forming galaxies: 240 Å which corresponds to $\mathcal{M} = 2.2$ in our models. For SFR$< 10^{-2}$ $M_\odot \mathrm{yr}^{-1}$, the low end of the PDF shows a bulkier shape that confirms the existence of systems with $\mathcal{M} < 1$ purely as a consequence of their intrinsic star formation stochasticity. We quantify and elaborate in the next section the implications of these results.

Table 1. Best fit values for the parameters used in the conditional PDF $P(\mathcal{M}|\text{SFR})$ (see Eq.4).

.

SFR $(\text{M}_\odot\text{yr}^{-1})$	$Z/Z_\odot$	$\mathcal{M}_0$	α	γ	P_0
0.0010	0.02	0.75±0.03	0.13±0.03	2.67±0.10	1.15±0.05
0.0015	0.02	0.71±0.02	0.44±0.03	2.73±0.09	1.44±0.04
0.0025	0.02	0.71±0.03	0.74±0.06	2.82±0.16	1.66±0.07
0.0040	0.02	0.76±0.01	1.03±0.03	3.49±0.09	1.86±0.03
0.0063	0.02	0.80±0.01	1.21±0.02	3.83±0.05	1.97±0.01
0.010	0.02	0.77±0.01	1.81±0.10	4.01±0.10	2.37±0.06
0.015	0.02	0.75±0.01	2.15±0.08	3.95±0.11	2.57±0.03
0.025	0.02	0.75±0.01	2.79±0.08	4.12±0.09	2.89±0.03
0.040	0.02	0.79±0.01	3.18±0.06	4.66±0.06	3.09±0.02
0.063	0.02	0.76±0.01	4.31±0.07	4.52±0.06	3.43±0.01
0.1	0.02	0.77±0.01	5.12±0.13	4.57±0.10	3.64±0.03
1.0	0.2	0.85±0.01	12.49±0.36	6.01±0.11	5.23±0.05
0.0010	0.2	0.64±0.05	0.013±0.040	2.25±0.15	1.20±0.10
0.0015	0.2	0.58±0.04	0.39±0.05	2.38±0.14	1.62±0.09
0.0025	0.2	0.64±0.02	0.62±0.04	2.73±0.12	1.72±0.06
0.0040	0.2	0.78±0.02	0.70±0.05	3.60±0.18	1.74±0.06
0.0063	0.2	0.71±0.01	0.70±0.05	3.62±0.14	2.10±0.05
0.010	0.2	0.69±0.01	1.52±0.07	3.96±0.15	2.50±0.05
0.015	0.2	0.72±0.01	1.85±0.09	4.34±0.18	2.61±0.06
0.025	0.2	0.64±0.01	3.08±0.11	3.90±0.09	3.30±0.03
0.040	0.2	0.70±0.01	2.87±0.13	4.50±0.17	3.26±0.05
0.063	0.2	0.71±0.01	3.46±0.16	4.87±0.19	3.58±0.05
0.1	0.2	0.70±0.01	4.42±0.13	4.69±0.10	3.93±0.03
1.0	0.2	0.76±0.01	11.52±0.43	6.08±0.15	5.87±0.07

4 DISCUSSION

4.1 High EW outliers and apparent Lymanα escape fraction

The ensuing discussion will focus on the interpretation of high and low EW systems that naturally emerge through stochasticity. High EW vales might lead one to propose the presence of very low metallicity (or population III) stars while low EW values could cause some galaxies not to be selected as a LAE in very deep narrowband surveys.

A common assumption in the search for galaxies with Population III stars is the following: there is an upper EW value to consider a star forming galaxy to be normal. This threshold value is taken to be $\text{EW}_{\text{th}} \sim 240$ Å but, as we show in the previous section, galaxies with similar or larger EW values can be expected by stochasticity effects without demanding Pop III stars. The threshold value $\text{EW}_{\text{th}} = 240$ Å corresponds to $\mathcal{M} = 2.2$ (Eq. 3). We can then quantify the fraction of such galaxies that have EW that exceed the threshold by using Eq. (4). For galaxies with star formation rates in the range 0.1–$1 \text{ M}_\odot\text{yr}^{-1}$ we find that there would be between $0.5 - 2.0\%$ of systems with EW values larger than EW_{th}. We calculate same fraction directly from the 500×10 points used to build the PDF and find that between 1% to 3% among them have an EW larger than EW_{th}.

This suggests that a minimal threshold in EW is not enough to assert that an individual galaxy presents signatures of population III stars. However, also the effects of stochasticity cannot be observationally evaluated from the measurement of an individual galaxy. Only statistical studies of galaxy samples are an appropriate tool to find clear signposts either of special stellar populations or stochasticity.

Narrowband surveys for LAEs often employ color cuts that can be approximated by requiring that the EW of a galaxy exceeds threshold value, which typically lies in the range $\text{EW}_{\text{cut}} = 20 - 65$ Å (see § 1). The result of previous sections show that low values of the SFR$< 10^{-2} \text{ M}_\odot \text{ yr}^{-1}$ the EW can be lower than half of the expected EW_0. In a survey that adopts color-cuts that correspond to a high EW_{cut}, one could simply miss those objects due to their low intrinsic EW. This shows how stochasticity can induce selection bias in LAEs observations.

Not surprisingly, the impact of stochasticity is highly SFR dependent. The strong dependence of the shape of the $\mathcal{M}$–PDF on SFR causes a larger fraction of systems to be found below a fixed $\mathcal{M}$ threshold for detection as the SFR decreases. In Figure 2 we show the fraction of LAEs that are missed as a function of the star formation rate, for different cuts in the EW expressed by EW_c. These fractions are calculated directly from the SLUG models, providing an uncertainty on the order of ~ 0.01 in the reported fraction of detected galaxies, the discrepancy of calculating the same fractions from the fitting function is in all cases smaller than ~ 0.02. The value of $\text{EW}_c = 20$ Å corresponds to a common cut used in present day observations (e.g. Ouchi et al. 2008). A cut of $\text{EW}_c = 50$ Å represents the cut used in the early observational attempts to find Lyman α emitting galaxies (e.g. Rhoads et al. 2000). In § 4.2 we investigate how such a bias may affect predicted number densities of LAEs in simplified (but often employed) models of LAEs.

4.2   The connection between the LAE-LF and the UV-LF

In this section we study the potential impact of stochasticity on the predicted Lyα luminosity functions & equivalent width distribution of narrowband selected galaxies (i.e. LAEs). We compare two very simple models to isolate and highlight the impact of stochasticity. In the first model we ignore stochastic ffects. We further assume that each star forming galaxy has a Lyα emission line with EW=EW$_0$ = 110 Å (see § 2). In the second model, we instead assume that the Lyα emission line of a star forming galaxy is drawn from a PDF which is set entirely by stochasticity effects. We therefore assume that the function $P(\text{EW}|\text{SFR})$ is given by Eq 4 for the second model. Finally, we further assume that there is a one-to-one correspondence between SFR and M_{UV} (given by the standard conversion factor between SFR and UV continuum flux, see § 2), and therefore[2] that $P(\text{EW}|\text{SFR}) \equiv P(\text{EW}|M_{\text{UV}})$. Under these assumptions, we can predict the LAE Lyα luminosity function, $\Psi(L_\alpha)$, for both models as (Dijkstra & Wyithe 2012)

$$\Psi(L_\alpha) = \ln 10 \int dM_{\text{UV}} \ \phi(M_{\text{UV}}) \times \text{EW}_{\text{c}} \times P(\text{EW}_{\text{c}}|M_{\text{UV}}), \quad (5)$$

where $\Psi(L_\alpha)d\log L_\alpha$ denotes the comoving number density of LAEs in the luminosity range $\log L_\alpha \pm d\log L_\alpha/2$. Furthermore, $\phi(M_{\text{UV}})$ denotes the comoving number density of star forming galaxies with absolute UV-magnitude in the range $M_{\text{UV}} \pm dM_{\text{UV}}/2$. The equivalent width EW$_{\text{c}}$ denotes the EW which corresponds to a Lyα line of luminosity L_α for an absolute UV magnitude M_{UV} (see Dijkstra & Wyithe 2012 for details). We focus our analysis on $z = 5.7$ and compare to the observed LAE Lyα luminosity functions at this redshift by Ouchi et al. (2008). We take the observed $\phi(M_{\text{UV}})$ at $z \sim 6$ from Bouwens et al. (2007) and 'rescale' it to $z = 5.7$ assuming that M^*_{UV} evolves with redshift as $M^*_{\text{UV}} = -21.02 + 0.36(z - 3.8)$ (Bouwens et al. 2008).

Figure 4.2 shows the luminosity function for the first model (no stochasticity) as the *black solid line*, and the second model (with stochasticity) as the *red dashed line*. The data points represent observations by Ouchi et al. (2008). Both models are remarkably similar. The reason for this similarity is non-trivial: stochasticity decreases the 'most likely' EW for star forming galaxies compared to models that do not include this effect (see Fig 1). This decrease alone would reduce the predicted Lyα luminosity functions. However, it is compensated for by the fact the $\mathcal{M}$-PDF has a tail to values $\mathcal{M} > 1$. The presence of this tail allows for an additional contribution to $\Psi(L_\alpha)$ (at a given L_α) by UV-faint galaxies that would not be able to contribute in the absence of stochasticity. Our prediction further assumes that $P(\text{EW}|\text{SFR} > 1 M_\odot \ \text{yr}^{-1})=P(\text{EW}|\text{SFR} = 1 M_\odot \ \text{yr}^{-1})$, and therefore likely overestimates the impact of stochasticity at SFR$> 1 M_\odot \ \text{yr}^{-1}$ (which corresponds to $L_\alpha > 10^{42} \ \text{erg s}^{-1}$). We therefore safely conclude that stochasticity barely im-

---

[2] Of course, in reality stochasticity introduces a dispersion in the value of SFR at a given M_{UV}, and the proper EW-PDF for a fixed M_{UV} is $P(\text{EW}|M_{\text{UV}}) = \int d \ \text{SFR} \ P(\text{EW}|\text{SFR})P(\text{SFR}|M_{\text{UV}})$. Because the PDF $P(\text{EW}|\text{SFR})$ varies relatively weakly with SFR, this proper calculation barely changes our results at all.
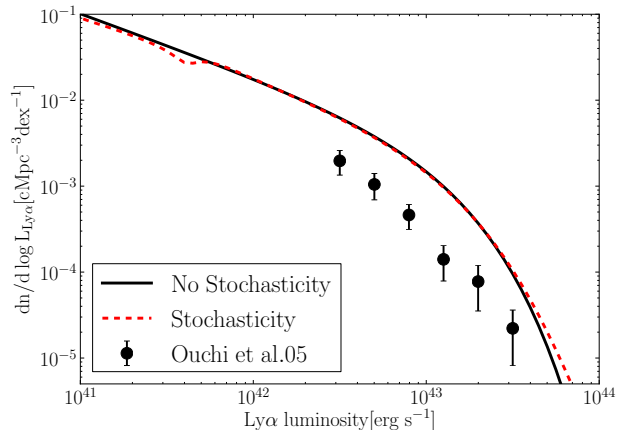

Figure 3. This Figure shows predicted Lyα luminosity function of LAEs for simplified models with (without) the effects of stochasticity included as the *red dashed* (*black solid line*). Also shown are the observations taken from Ouchi et al. (2008, *black filled circles*). The main point of this plot is that stochasticity barely affects the predicted luminosity functions. Both models predict more LAEs than is observed, as we have not attempted to correct for dust extinction and/or intergalactic scattering, which would both reduce the predicted luminosity functions.

pacts predictions of Lyα luminosity functions. This result is not sensitive to the uncertainties in the fitting functions for the PDF($\mathcal{M}|\text{SFR}$) used here. Also shown for completeness is the observed $z = 5.7$ LAE luminosity function from Ouchi et al. (2008). Both models clearly predict more LAEs than is observed. This is not surprising as we have not attempted to correct for dust extinction and/or intergalactic scattering. Both these effects likely reduce the predicted Lyα luminosity at a fixed number density of objects, which would bring down the predicted luminosity functions.

The EW-PDF for a sample of Lyα-selected galaxies is given by (Dijkstra & Wyithe 2012)

$$P(\text{EW}|\log L_{\alpha,\text{min}}, \log L_{\alpha,\text{max}}) =$$
$$\mathcal{N} \int_{\log L_{\alpha,\text{min}}}^{\log L_{\alpha,\text{max}}} P(\text{EW}|M_{\text{UV,c}})\phi(M_{\text{UV,c}})d\log_{10} L_\alpha, \quad (6)$$

where $L_{\alpha,\text{min}}$ ($L_{\alpha,\text{max}}$) denotes the minimum (maximum) Lyα luminosity of the galaxies in the sample. Furthermore, $M_{\text{UV,c}}$ denotes the UV magnitude for which a Lyα line of luminosity L_α corresponds to an equivalent width EW (again see Dijkstra & Wyithe 2012 for details). We focus on the impact of stochasticity on the predicted PDF for $\log L_{\alpha,\text{min}} = 42$ and $\log L_{\alpha,\text{max}} = 43$ (*blue dotted line* (which corresponds approximately to 1 $M_\odot \ \text{yr}^{-1} <SFR< 10 \ M_\odot \ \text{yr}^{-1}$, and roughly to the range of observed Lyα luminosities). For comparison, we also show a case with $\log L_{\alpha,\text{min}} = 40$ and $\log L_{\alpha,\text{max}} = 42$ (*red dashed line*, which corresponds approximately to 0.01 $M_\odot \ \text{yr}^{-1} <SFR< 1 \ M_\odot \ \text{yr}^{-1}$). The choice $\log L_{\alpha,\text{min}} = 40$ is a bit arbitrary, but was motivated by the notion that galaxies with SFR$\sim 10^{-2} \ M_\odot \ \text{yr}^{-1}$ can contribute significantly to the overall ionizing photon budget during the Epoch of Reionization (see Kuhlen & Faucher-Giguere 2012).

The *black solid line* in Figure 4.2 shows the predicted EW-PDF for the model with no stochastic effects (which is
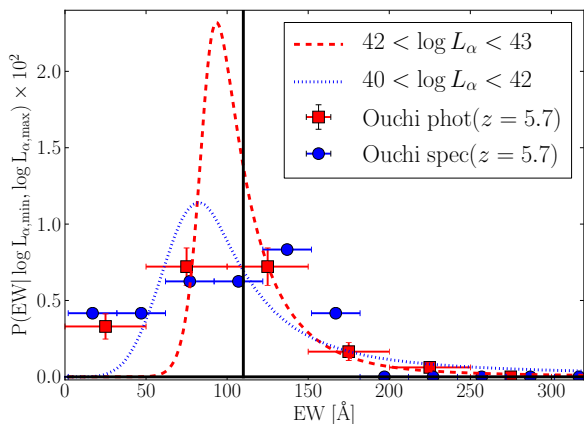
Figure 4. This Figure shows the predicted EW-PDF for a sample of Lyα selected galaxies. The *solid black line* shows the Dirac delta function for the model with no stochasticity effects. The *red dashed line* (*blue dotted line*) shows the predicted EW-PDF for models which include stochasticity effects for Lyα selected galaxies with $L_\alpha = 10^{40} - 10^{42}$ erg s^{-1} ($L_\alpha = 10^{42} - 10^{43}$ erg s^{-1}, see text). Also shown for comparison is the EW-PDF observed by Ouchi et al. (2008; the *red filled circles* represent their photometric data, while the *blue filled circles* represent their spectroscopic sample). This Figure illustrates that stochasticity may help explain the large observed values of EW of LAEs at z=5.7, although it fails to fully explain the observed EW-PDF.

simply a delta-function). The predicted PDF for the models that include stochasticity peak at the lower values of EW, and have tails that extend to values that greatly exceed EW= 100 Å. Also shown is the observed EW-PDF for a sample of photometrically selected (*red filled squares*) and spectroscopically confirmed (*blue filled circles*, taken from Ouchi et al. 2008) LAEs. Clearly, stochastic effects may help to explain large observed values of EW. However, additional processes such as dust extinction and/or intergalactic scattering, which impacts differently the UV continuum and the Lyα line (Forero-Romero et al. 2011), are needed to fully explain the observed EW-PDF of LAEs at z=5.7.

4.3 Stochastic effects on the Lyman continuum

The distribution of EW at a given averaged SFR is the result of fluctuations in the fluxes of ionizing and far UV continuum (non ionizing) photons. The ionizing photon production is dominated by short–lived O & B stars, while less massive A stars can contribute significantly to the non-ionizing photon flux. Because of the different lifetimes of these stars of different masses, the ionizing and non ionizing fluxes – and therefore their ratio – vary on different timescales and with different amplitudes.

Simultaneous fluctuations in the ionizing and non-ionizing fluxes can thus impact observational estimates of the ionizing escape fraction, which is usually estimated from a *relative escape fraction*:

$$f_{\text{esc,rel}} = \frac{(f_{\text{LyC}}/f_{1500})_{\text{obs}}}{(f_{\text{LyC}}/f_{1500})_{\text{stel}}} \exp\left(\tau_{\text{IGM}}\right), \qquad (7)$$

where the $(f_{\text{LyC}}/f_{1500})_{\text{stel}}$ is the intrinsic flux ratio for

a stellar population model, $(f_{\text{LyC}}/f_{1500})_{\text{obs}}$ is the observed flux ratio and τ_{IGM} is the LyC optical depth of the IGM at the redshift of emission.

Based on Subaru/Suprime-Cam imaging Iwata et al. (2009) claimed a detection of 10 LAEs and 3 LBGs at $z \sim 3.1$ with a significant emission in LyC out of a sample of 125 LAEs and 73 LBGs. Recent measurements seem to confirm such measurement for 8 LAEs using spectroscopy with VLT/VIMOS and SUBARU/FOCAS. The results indicate a LyC excess with respect to non-ionizing UV at ~ 1500Å expected by standard stellar populations (Inoue et al. 2011). However, observation targeting LyC in LBGs at $z \sim 1.3$ using deep Hubble Space Telescope imaging do not find any excess (Siana et al. 2010).

The sources present an excess of a factor of $\sim 2-3$ times larger than the expected intrinsic stellar ratio for f_{LyC}/f_{1500}. Some theoretical analysis requires a very top heavy IMF to explain the observed ratios or fractions of 10% in mass of very young < 1 Myr of extremely metal poor $Z < 1.0 \times 10^{-4}Z_\odot$ or metal free stellar populations (Inoue 2010; Inoue et al. 2011)

The stochasticity effects present an important element to be considered in such analysis: The ratio $\mathcal{M}$ can be directly interpreted as the excess of the f_{LyC}/f_{1500} ratio with respect to the constant expected value. The star formation rates for the objects with LyC excess are on the order of ~ 1 M$_\odot$ yr^{-1} ($M_{\text{UV}} \gtrsim -19$, see Fig 5 of Siana et al. 2010 and where we ignore dust in the conversion from M_{UV} to SFR). In this range $10 \pm 1\%$ of the galaxies will show an excess $1.5 - 2.0$ times the expected stellar f_{LyC}/f_{1500} ratio only due to stochasticity (Figure 1), this is consistent with the fraction of galaxies observed with those characteristics.

The stochasticity might also explain why the LyC excess is not observed in the recent $z \sim 1.3$ Hubble imaging by Siana et al. (2010). The LBGs observed at that redshift have systematically restframe magnitudes $M_{\text{UV}} < -20$, while the LyC excess sources are fainter than this limit. This transition roughly corresponds to a SFR ~ 5 M$_\odot$ yr^{-1} assuming a standard conversion factor, while the fainter systems reported with an excess have $M_{\text{UV}} \sim -18$ and SFR ~ 1 M$_\odot$ yr^{-1}. The dependence of the stochasticity effects on the SFR make it more likely to detect the LyC excess in the fainter sample. Probably the stronger effect is of statistic origin, given that the observations at $z \sim 1.3$ target 15 LBGs, while at $z \sim 3.0$ a set of 198 galaxies were observed, this provides one order of magnitude less objects to sample the $P(\mathcal{M})$ distribution and find galaxies with a LyC excess.

5 CONCLUSIONS

In this paper we have investigated the quantitative impact of stochastic sampling of the stellar initial mass function (IMF) on the Lyα, and ionizing photon emissivity of dwarf galaxies. We have used the SLUG code to simulate the spectral energy distribution for restframe wavelengths $\lambda \lesssim 2000$ Å of galaxies with time-averaged star formation rates in the range $(10^{-3} - 1)$ M$_\odot$ yr^{-1}.

From our predicted Far UV continuum flux density (at $\langle\lambda\rangle = 1500$ Å) and the ionizing flux density (at $\langle\lambda\rangle < 912$ Å) we construct probability distribution function (PDF) for the variable $\mathcal{M}$ that represents the ratio of the measured

restframe equivalent width (EW) of the Lyα line to the expected constant value in the absence of stochasticity (EW$_0$), i.e. $\mathcal{M} \equiv$ EW/EW$_0$.

We find that the $\mathcal{M}$–PDF can be represented by a double power law in $\mathcal{M}$, whose parameters are highly dependent on the SFR. We emphasize that the results derived from these experiments are sensitive to the degree of the clustering properties of the stars. In the case of $f_c = 0$ where the star formation is completely unclustered, the dispersion around the mean is reduced by a factor of 10 (da Silva et al. 2012). The results are also sensitive to the star formation history assumed: in the case of a bursty star formation history, one could expect the scatter around the mean for $\mathcal{M}$ to be higher than what we derive here.

Our results show that it is possible for galaxies to have both extremely low and high $\mathcal{M}$ values – especially at increasingly low SFR – and investigate implications of this result. In particular, we show how the existence of galaxies with low $\mathcal{M}$ values can induce an observational bias if galaxies are selected by cuts in the equivalent width (as in narrowband surveys for LAEs). This bias may cause dwarfs with lower SFRs < 0.1 M$_\odot$yr^{-1} more likely to be missed in narrowband surveys. On the other hand, the existence of galaxies with high $\mathcal{M}$ implies that a high EW cannot unambiguously be interpreted as a defining characteristic of primordial population III galaxies (Schaerer 2003; Johnson et al. 2009; Pawlik et al. 2011). Finally, we use the framework presented in Dijkstra & Wyithe 2012 to quantify the impact of stochasticity on the predicted luminosity function and EW-PDF of a sample of Lyα emitters (LAEs, i.e. narrowband selected galaxies) at a fixed redshift. We find that while stochasticity does not appreciably affect the LAE abundance modeling, it may help to explain the large EW (EW $\gtrsim 100 - 200$ Å) observed for a fraction of LAEs.

Finally, we have also shown that stochasticity can affect inferred constraints on the escape fraction of ionizing radiation, most strongly in galaxies that form stars at rates SFR $\lesssim 1 M_\odot$ yr^{-1}. Given that such galaxies are thought to dominate the reionization process at $z > 6$, it is important to consider the effects of stochasticity when using 'local' observations to put constraints on their ionizing luminosities and escape fractions. In particular, the observed anomalies in the ratio of LyC to non-ionizing UV radiation in so-called 'Lyman-Bump' galaxies at $z = 3.1$ reported by Iwata et al. (2009) can be explained naturally in the context of the stochastic sampling of the IMF, without resorting to unusual stellar populations. Moreover, the absence of such objects in a sample of 15 LBGs at $z \sim 1.3$ (Siana et al. 2010) is also expected as these galaxies are forming stars at rates at which the stochastic sampling of the IMF becomes negligible.

REFERENCES

Barkana R., Loeb A., 2001, PhR, 349, 125

Bouwens R. J., Illingworth G. D., Franx M., Ford H., 2007, ApJ, 670, 928

Bouwens R. J., Illingworth G. D., Franx M., Ford H., 2008, ApJ, 686, 230

da Silva R. L., Fumagalli M., Krumholz M., 2012, ApJ, 745, 145

Dayal P., Ferrara A., 2012, MNRAS, 421, 2568

Dijkstra M., Mesinger A., Wyithe J. S. B., 2011, MNRAS, 414, 2139

Dijkstra M., Westra E., 2010, MNRAS, 401, 2343

Dijkstra M., Wyithe J. S. B., 2012, MNRAS, 419, 3181

Dunlop J. S., McLure R. J., Robertson B. E., Ellis R. S., Stark D. P., Cirasuolo M., de Ravel L., 2012, MNRAS, 420, 901

Finkelstein S. L., Papovich C., Salmon B., Finlator K., Dickinson M., Ferguson H. C., Giavalisco M., Koekemoer A. M., Reddy N. A., Bassett R., Conselice C. J., Dunlop J. S. e. a., 2011, ArXiv e-prints

Forero-Romero J. E., Yepes G., Gottlöber S., Knollmann S. R., Cuesta A. J., Prada F., 2011, MNRAS, 415, 3666

Forero-Romero J. E., Yepes G., Gottlöber S., Prada F., 2012, MNRAS, 419, 952

Fumagalli M., da Silva R. L., Krumholz M. R., 2011, ApJL, 741, L26

Haas M. R., Anders P., 2010, A&A, 512, A79

Hillier D. J., Miller D. L., 1998, ApJ, 496, 407

Inoue A. K., 2010, MNRAS, 401, 1325

Inoue A. K., Kousai K., Iwata I., Matsuda Y., Nakamura E., Horie M., Hayashino T., Tapken C., Akiyama M., Noll S., Yamada T., Burgarella D., Nakamura Y., 2011, MNRAS, 411, 2336

Iwata I., Inoue A. K., Matsuda Y., Furusawa H., Hayashino T., Kousai K., Akiyama M., Yamada T., Burgarella D., Deharveng J.-M., 2009, ApJ, 692, 1287

Johnson J. L., Greif T. H., Bromm V., Klessen R. S., Ippolito J., 2009, MNRAS, 399, 37

Kennicutt Jr. R. C., 1998, ARA&A, 36, 189

Kuhlen M., Faucher-Giguere C.-A., 2012, ArXiv e-prints

Leitherer C., Schaerer D., Goldader J. D., González Delgado R. M., Robert C., Kune D. F., de Mello D. F., Devost D., Heckman T. M., 1999, ApJS, 123, 3

Lejeune T., Cuisinier F., Buser R., 1997, A&AS, 125, 229

Lejeune T., Cuisinier F., Buser R., 1998, A&AS, 130, 65

Mesinger A., 2010, MNRAS, 407, 1328

Ono Y., Ouchi M., Mobasher B., Dickinson M., Penner K., Shimasaku K., Weiner B. J., Kartaltepe J. S., Nakajima K., Nayyeri H., Stern D., Kashikawa N., Spinrad H., 2012, ApJ, 744, 83

Ouchi M., Shimasaku K., Akiyama M., Simpson C., Saito T., Ueda Y., Furusawa H., Sekiguchi K., Yamada T., Kodama T., Kashikawa N., Okamura S., Iye M., Takata T., Yoshida M., Yoshida M., 2008, ApJS, 176, 301

Pawlik A. H., Milosavljević M., Bromm V., 2011, ApJ, 731, 54

Pentericci L., Fontana A., Vanzella E., Castellano M., Grazian A., Dijkstra M., Boutsia K., Cristiani S., Dickinson M., Giallongo E., Giavalisco M., Maiolino R., Moorwood A., Paris D., Santini P., 2011, ApJ, 743, 132

Pritchard J. R., Loeb A., Wyithe J. S. B., 2010, MNRAS,

408, 57

Raiter A., Schaerer D., Fosbury R. A. E., 2010, A&A, 523, A64

Rhoads J. E., Malhotra S., Dey A., Stern D., Spinrad H., Jannuzi B. T., 2000, ApJL, 545, L85

Robertson B. E., Ellis R. S., Dunlop J. S., McLure R. J., Stark D. P., 2010, Nature, 468, 49

Schaerer D., 2003, A&A, 397, 527

Schenker M. A., Stark D. P., Ellis R. S., Robertson B. E., Dunlop J. S., McLure R. J., Kneib J.-P., Richard J., 2012, ApJ, 744, 179

Shimizu I., Yoshida N., Okamoto T., 2011, MNRAS, 418, 2273

Siana B., Teplitz H. I., Ferguson H. C., Brown T. M., Giavalisco M., Dickinson M., Chary R.-R., de Mello D. F., Conselice C. J., Bridge C. R., Gardner J. P., Colbert J. W., Scarlata C., 2010, ApJ, 723, 241

Smith L. J., Norris R. P. F., Crowther P. A., 2002, MNRAS, 337, 1309

Stark D. P., Ellis R. S., Chiu K., Ouchi M., Bunker A., 2010, MNRAS, 408, 1628

Stark D. P., Ellis R. S., Ouchi M., 2011, ApJL, 728, L2

Steidel C. C., Giavalisco M., Pettini M., Dickinson M., Adelberger K. L., 1996, ApJL, 462, L17